

# Convective heat transport in a rotating fluid layer of infinite Prandtl number: Optimum fields and upper bounds on Nusselt number

Nikolay K. Vitanov\*

*Institute of Mechanics, Bulgarian Academy of Sciences Akad. G. Bonchev Street, Block 4, 1113 Sofia, Bulgaria and Max-Planck-Institute for Physics of Complex Systems, Noethnitzerstrasse 38, D-01187 Dresden, Germany*

(Received 8 April 2002; published 27 February 2003)

By means of the Howard-Busse method of the optimum theory of turbulence we investigate numerically upper bounds on convective heat transport for the case of infinite fluid layer with stress-free vertical boundaries rotating about a vertical axis. We discuss the case of infinite Prandtl number,  $1 - \alpha$  solution of the obtained variational problem and optimum fields possessing internal, intermediate, and boundary layers. We investigate regions of Rayleigh and Taylor numbers  $R$  and  $Ta$ , where no analytical bounds can be derived, and compare the analytical and numerical bounds for these regions of  $R$  and  $Ta$  where such comparison is possible. The increasing rotation has a different influence on the rescaled optimum fields of velocity  $w_1$ , temperature  $\theta_1$  and the vertical component of the vorticity  $f_1$ . The increasing  $Ta$  for fixed  $R$  leads to vanishing of the boundary layers of  $w_1$  and  $\theta_1$ . Opposite to this, the increasing  $Ta$  leads first to a formation of boundary layers of the field  $f_1$  but further increasing the rotation causes vanishing of these boundary layers. We obtain optimum profiles of the horizontal averaged total temperature field which could be used as hints for construction of the background fields when applying Doering-Constantin method to the problems of rotating convection. The wave number  $\alpha_1$  corresponding to the optimum fields follows the asymptotic relationship  $\alpha_1 = (R/5)^{1/4}$  for intermediate Rayleigh numbers. However, when  $R$  becomes large with respect to  $Ta$ , after a transition region, the power law for  $\alpha_1$  becomes close to the power law for the case without rotation. The Nusselt number  $Nu$  is close to the nonrotational bound  $0.32R^{1/3}$  for the case of large  $R$  and small  $Ta$ .  $Nu$  decreases with increasing Taylor number. Thus, the upper bounds reflect the tendency of inhibiting thermal convection by increasing rotation for a fixed Rayleigh number. For the regions of Rayleigh and Taylor numbers where the numerical and asymptotic bounds on  $Nu$  can be compared, the numerical bounds are about 70% lower than the asymptotic bounds.

DOI: 10.1103/PhysRevE.67.026322

PACS number(s): 47.27.Te, 47.27.Cn

## I. INTRODUCTION

The turbulent solutions of the Navier-Stokes equations at very large Reynolds or Rayleigh numbers are extremely complicated. The optimum theory of turbulence is among a small number of tools for obtaining rigorous estimates of the turbulent quantities directly from these equations. It leads to upper bounds on turbulent quantities on the basis of or integral constraints which are members of infinite system of moment equations. Using finite number of these integral constraints, we determine the class of fields among which the upper-bound solution of the corresponding variational problem is sought. All solutions of the Navier-Stokes equations are contained in this class of fields and in addition the energy balance of the real flow is retained. We can restrict the number of considered fields by taking into account additional constraints. Thus, in principle, we can tighten the upper bounds on the investigated quantities.

Two methods of the optimum theory of turbulence are known. The Howard-Busse method is based on the ideas of Malkus [1,2], variational approach of Howard [3], and the multi- $\alpha$ -solutions of Busse [4]. This method was successfully used by Chan [5] and applied to many cases of fluid flows and thermal convection [7–22]. We mention the recent success in lowering the bounds on convective heat transport

for convection in a rotating layer of finite Prandtl number through the use of separate energy balances for toroidal and poloidal components of velocity field [21].

Another interesting method of the optimum theory of turbulence was proposed by Doering and Constantin [23]. This method and its modification [24] are based on the idea for a decomposition of the velocity field into a steady background field that satisfies the inhomogeneous boundary conditions, and a homogeneous fluctuations field. An appropriate background field that satisfies certain spectral constraints easily leads to an upper bound on the corresponding turbulent quantity [25–46]. In addition to the application for different flows and thermal convection the optimum theory of turbulence was applied in plasma physics for obtaining upper bounds on the heat transport due to the ion-temperature gradient, on the energy dissipation in a turbulent pinch, etc. [47–53].

Many phenomena in earth atmosphere, oceans, solar, and planetary atmospheres are based on the turbulent thermal convection in presence of rotation. Thus, it is a subject of extensive theoretical and experimental investigations [54–68]. In this paper we use the Howard-Busse method of the optimum theory of turbulence and obtain numerical upper bounds on convective heat transport in a horizontal layer of fluid rotating about a vertical axis for the case of moderate rotation rates and stress-free boundaries. The analytical treatment of this problem has been presented in Refs. [8,69]. A discussion of the problem of rotating convection from the

\*Electronic address: vitanov@imech.imbm.bas.bg

point of view of the Doering-Constantin method is presented in Refs. [37,44,45].

Numerical investigations are extremely useful in the optimum theory of turbulence because of the following reasons.

(a) In contrast to the analytical theory, by means of numerical investigation we obtain profiles of optimum fields and bounds on the turbulent quantities without any assumptions concerning the Euler-Lagrange equations of the variational problem. The only limitation on the size of the region of the obtained bounds in the  $R$ - $Ta$  plane is the computer power.

(b) If we are able to reach the regions of large Rayleigh and Taylor numbers, we can test the assumptions of the analytical asymptotic theory, to correct them and to amend the theory if necessary.

(c) The obtained numerical bounds are important also for small and intermediate values of the Rayleigh and Taylor numbers where the assumptions of the asymptotic theory are not valid. Our experience [15,16,20] shows that the numerical bounds are lower than the analytical asymptotic bounds for large Rayleigh numbers.

(d) For very large values of Rayleigh and Taylor numbers, the numerical bounds approach the asymptotic bounds from below. If we are able to obtain numerical solutions for such large values of the Rayleigh and Taylor numbers, we can try to extract directly the asymptotic laws for the Nusselt number or for the wave numbers of the optimum fields.

(e) For many problems, we wish to develop an asymptotic theory based on the multi- $\alpha$  solutions of the variational problem. In order to do this successfully, we have to understand the asymptotic behavior of the optimum fields as well as the asymptotic behavior of the bound on the convective heat transport for the case of  $1-\alpha$  solution of the corresponding variational problem. This makes the numerical investigation of the corresponding  $1-\alpha$  solution of the variational problem very important.

In this paper, we obtain numerically profiles of optimum fields and upper bounds on the Nusselt number for the case when the optimum fields consist of internal, intermediate, and boundary layers. We restrict the investigation to the case of one wave number of the optimum fields with an objective to test the assumptions of the recently presented asymptotic theory [69], and to pave the way for constructing analytical multi-wave-number theory, which eventually will lead to correction of Chan's bounds [8]. It has been shown [19,69] that the bounds of Chan are upper bounds on the upper bounds on the Nusselt number for several cases of convection with and without rotation. We could expect a similar result also for the multi-wave-number bounds for the rotating convection. The rotation leads to enormous complication in the analytical treatment of the multi-wave-number bounds. To avoid mistakes, the theoretical assumptions must be very carefully checked for the case of the single-wave-number theory. This can be done numerically and it is performed in the following sections of the paper. In Sec. II, we formulate the variational problem and discuss the region of validity of the  $1-\alpha$  solution of the variational problem as a maximizing solution. In Sec. III, we discuss the investigated regions for Rayleigh and Taylor numbers and the behavior of the opti-

num fields. We show that these fields tend to satisfy the assumptions of the analytical asymptotic theory with increasing Rayleigh and Taylor numbers. We investigate the complicated behavior of the optimum field connected to the vertical component of vorticity. In addition, we obtain optimum profiles of horizontally averaged temperature field. Sec. IV is devoted to the behavior of the optimum heat transport and corresponding wave number. Several concluding remarks are presented in Sec. V.

## II. MATHEMATICAL FORMULATION OF THE PROBLEM

We investigate a horizontal layer of fluid heated from below, which rotates about the vertical axis with a constant angular velocity  $\Omega$ . Let us discuss the idealized situation of an infinite layer and consider the Boussinesq approximation to the equations of the fluid flow [70]. We shall use the following notations.  $d$ , thickness of the fluid layer;  $\kappa$ , thermometric conductivity of the fluid;  $\nu$ , kinematic viscosity of the fluid;  $g$ , acceleration of the gravity;  $\Delta T$ , the temperature difference between the upper and lower fluid boundary;  $\rho$ , density of the fluid;  $P = \nu/\kappa$ , Prandtl number;  $Ta = (2\Omega d^2/\nu)^2$ , Taylor number;  $R = (\gamma g \Delta T d^3)/(\kappa \nu)$ , Rayleigh number;  $\gamma$ , coefficient of thermal expansion;  $p$ , pressure; and  $\mathbf{k}$ , unit vector in the direction opposite to the gravity.

Denoting the horizontal size of the fluid layer as  $L$ , we define averages of quantities over the planes  $z = \text{const}$  and over the fluid layer

$$\bar{q} = \lim_{L \rightarrow \infty} \frac{1}{4L^2} \int_{-L}^L \int_{-L}^L dx dy \{q(x, y, z, t)\}, \quad (1)$$

$$\langle q \rangle = \lim_{L \rightarrow \infty} \frac{1}{4L^2} \int_{-L}^L \int_{-L}^L \int_{-1/2}^{1/2} dx dy dz \{q(x, y, z, t)\}. \quad (2)$$

Taking  $d$  as a unit for length,  $\kappa/d$  as unit for velocity,  $d^2/\kappa$  as unit for time, and  $\rho \nu \kappa/d^2$  as unit for pressure, we obtain the dimensionless form of the Boussinesq equations,

$$\frac{1}{P} \left( \frac{\partial \mathbf{u}}{\partial t} + \mathbf{u} \cdot \nabla \mathbf{u} \right) = -\frac{\sqrt{Ta}}{2} \nabla p + \nabla^2 \mathbf{u} + RT \mathbf{k} + \sqrt{Ta} (\mathbf{u} \times \mathbf{k}), \quad (3)$$

$$\frac{\partial \Theta}{\partial t} + \mathbf{u} \cdot \nabla \Theta = \nabla^2 \Theta, \quad (4)$$

$$\nabla \cdot \mathbf{u} = 0. \quad (5)$$

The boundary conditions at  $z = \pm 1/2$  are stress-free:  $u_3 = \partial^2 u_3 / \partial z^2 = T = 0$ . The quantity  $\Theta$  in Eq. (4) is the total temperature field and  $T$  is the deviation of the temperature field from its horizontal mean.

$$\Theta = \bar{\Theta} + T. \quad (6)$$

We formulate a variational problem using two moment equations obtained on the basis of the Boussinesq equations.

We assume that (i) all necessary horizontal averages of the functions, describing the flow exist, (ii) the horizontal averages of the fluctuation quantities vanish, (iii) the flow is statistically steady in time and homogeneous in the horizontal averages.

Our objective is to obtain an upper bound on the convective heat transport through the fluid layer, i.e., upper bound on the Nusselt number

$$\text{Nu} = 1 + \frac{\langle u_3 T \rangle}{R}. \quad (7)$$

We introduce Eq. (6) in the Boussinesq equations, multiply Eq. (3) by the velocity  $\mathbf{u}$ , and average over the fluid layer. The result is a relationship known also as a power integral

$$\langle |\nabla \cdot \mathbf{u}|^2 \rangle = R \langle u_3 T \rangle. \quad (8)$$

Another relationship can be obtained by a multiplication of Eq. (4) by  $T$  and by averaging the result over the fluid layer. In this way, we obtain a relationship containing the term  $\langle u_3 T (\partial \bar{\Theta} / \partial z) \rangle$ . It can be transformed by a horizontal averaging of the heat equation and integrating the obtained result with respect to  $z$ . Thus, we obtain

$$\frac{d\bar{\Theta}}{dz} = \overline{u_3 T} - \langle u_3 T \rangle - 1, \quad (9)$$

and the second power integral

$$\langle |\nabla T|^2 \rangle = \langle u_3 T \rangle^2 - \overline{\langle u_3 T^2 \rangle} + \langle u_3 T \rangle. \quad (10)$$

By means of Eq. (9), we shall calculate the mean temperature  $\bar{\Theta}$  in the following section. The assumption of infinite Prandtl number allows us to include additional restrictions on the manifold of candidates for optimum fields. Our investigations [21] show that the upper bound on convective heat transport in the case of a horizontal fluid layer heated from below and rotating about a vertical axis depends weakly on the Prandtl number when the Prandtl number is close to 7 and larger. This defines the region of Prandtl numbers, for which the approximation of infinite Prandtl number, used here, is valid.

When Prandtl number is infinite, the Navier-Stokes equation becomes linear and we include it as a constraint in the variational problem. We take into account the equation of continuity by the general representation of a solenoidal field  $\mathbf{u}$  in terms of a poloidal and a toroidal component

$$\mathbf{u} = \nabla \times (\nabla \times \mathbf{k} \phi) + \nabla \times \mathbf{k} \psi. \quad (11)$$

We introduce Eq. (11) into the Navier-Stokes equation ( $P = \infty$ ) and perform the rescalings

$$\mathbf{u} = \mu^{1/2} \langle w \theta \rangle^{-1/2} \mathbf{v}, \quad T = \mu^{1/2} \langle w \theta \rangle^{-1/2} R^{-1} \theta, \quad (12)$$

where  $z$  component of the rescaled velocity field  $\mathbf{v}$  is denoted as  $w$ . Taking the  $z$  component of the horizontal curl and the  $z$  component of the double curl of the result, we obtain the relationships

$$\nabla^2 f + \sqrt{\text{Ta}} \frac{\partial w}{\partial z} = 0, \quad (13)$$

$$\nabla^4 w + \nabla_1^2 \theta - \sqrt{\text{Ta}} \frac{\partial f}{\partial z} = 0, \quad (14)$$

where  $f = -\nabla_1 \psi$  is the vertical component of the vorticity. Substitution of Eq. (12) in Eq. (10) leads to

$$R = \frac{\langle |\nabla \theta|^2 \rangle}{\langle w \theta \rangle} + \mu \frac{\langle (\overline{w \theta} - \langle w \theta \rangle)^2 \rangle}{\langle w \theta \rangle^2}. \quad (15)$$

Using Eqs. (13), (14), and (15), we formulate the following variational problem ( $p^*$  and  $q^*$  are Lagrange multipliers): *Find the minimum  $R(\mu)$  of the variational functional*

$$\begin{aligned} \mathcal{R} = & \frac{\langle |\nabla \theta|^2 \rangle}{\langle w \theta \rangle} + \mu \frac{\langle (\overline{w \theta} - \langle w \theta \rangle)^2 \rangle}{\langle w \theta \rangle^2} - \left\langle p^* \left( \nabla^2 f + \sqrt{\text{Ta}} \frac{\partial w}{\partial z} \right) \right\rangle \\ & - \left\langle q^* \left( \nabla^4 w + \nabla_1^2 \theta - \sqrt{\text{Ta}} \frac{\partial f}{\partial z} \right) \right\rangle, \end{aligned} \quad (16)$$

among all fields  $w$ ,  $\theta$ ,  $f$  that satisfy the boundary conditions

$$w = \theta = \frac{\partial^2 w}{\partial z^2} = \frac{\partial f}{\partial z} = 0, \quad (17)$$

at  $z = \pm 1/2$ .

The corresponding Euler-Lagrange equations are Eqs. (13), (14), and

$$\begin{aligned} \langle |\nabla \theta|^2 \rangle \theta + 2 \theta [\mu (\overline{w \theta} - \langle w \theta \rangle) - R \langle w \theta \rangle] \\ - \langle w \theta \rangle^2 \left( \nabla^4 q^* - \sqrt{\text{Ta}} \frac{\partial p^*}{\partial z} \right) = 0, \end{aligned} \quad (18)$$

$$\begin{aligned} \langle |\theta|^2 \rangle w - 2 \langle w \theta \rangle \nabla^2 \theta + 2 w [\mu (\overline{w \theta} - \langle w \theta \rangle) - R \langle w \theta \rangle] \\ - \langle w \theta \rangle^2 \nabla_1^2 q^* = 0, \end{aligned} \quad (19)$$

$$\nabla^2 p^* + \sqrt{\text{Ta}} \frac{\partial q^*}{\partial z} = 0. \quad (20)$$

We note that the fields  $w$  and  $\theta$ , determined from the Euler-Lagrange equations, automatically satisfy the power integral (8). After elimination of the Lagrange multipliers and introduction the  $1 - \alpha$  solutions of the variational problem,

$$w = w_1(z) \phi(x, y), \quad (21)$$

$$\theta = \theta_1(z) \phi(x, y), \quad (22)$$

$$f = f_1(z) \phi(x, y), \quad (23)$$

where  $\overline{\phi\phi}=1$  and  $\nabla_1^2\phi=-\alpha_1^2\phi$ , we obtain the following form of the Euler-Lagrange equations:

$$\begin{aligned}
 & 2\langle w_1\theta_1\rangle\left(\frac{d^2}{dz^2}-\alpha_1^2\right)^4\theta_1+\left[2\left(\frac{d^2}{dz^2}-\alpha_1^2\right)^3w_1\right. \\
 & \left.-\text{Ta}^{1/2}\left(\frac{d^2}{dz^2}-\alpha_1^2\right)\frac{df_1}{dz}\right]\left[2R\langle w_1\theta_1\rangle+\left\langle\theta_1\left(\frac{d^2}{dz^2}-\alpha_1^2\right)\theta_1\right\rangle\right] \\
 & -2\mu\alpha_1^2\left\{\left(\frac{d^2}{dz^2}-\alpha_1^2\right)[\theta_1(w_1\theta_1-\langle w_1\theta_1\rangle)]\right\}-2\mu\left\{\left(\frac{d^2}{dz^2}\right.\right. \\
 & \left.\left.-\alpha_1^2\right)^3[w_1(w_1\theta_1-\langle w_1\theta_1\rangle)]+\text{Ta}\frac{d^2w_1}{dz^2}\left\langle\theta_1\left(\frac{d^2}{dz^2}\right.\right.\right. \\
 & \left.\left.\left.-\alpha_1^2\right)\theta_1\right\rangle+2\text{Ta}\langle w_1\theta_1\rangle\right. \\
 & \left.\times\left(\frac{d^2}{dz^2}-\alpha_1^2\right)\frac{d^2\theta_1}{dz^2}-2\text{Ta}\frac{d^2}{dz^2}\{w_1[\mu(w_1\theta_1-\langle w_1\theta_1\rangle)]\right.\right. \\
 & \left.\left.-R\langle w_1\theta_1\rangle\right]\right\}=0, \tag{24}
 \end{aligned}$$

$$\left(\frac{d^2}{dz^2}-\alpha_1^2\right)f_1+\text{Ta}^{1/2}\frac{dw_1}{dz}=0, \tag{25}$$

$$\left(\frac{d^2}{dz^2}-\alpha_1^2\right)^2w_1-\alpha_1^2\theta_1=\text{Ta}^{1/2}\frac{df_1}{dz}. \tag{26}$$

The homogeneity of the Euler-Lagrange equations allows us to impose the requirement  $\mu=\langle w_1\theta_1\rangle$ . For  $w_1$ ,  $\theta_1$ , and  $f_1$ , we use the following relationships that satisfy the boundary conditions:

$$w_1(z)=\sum_{m=1}^M a_m\sin[(2m-1)\pi(z+1/2)], \tag{27}$$

$$\theta_1(z)=\sum_{m=1}^M b_m\sin[(2m-1)\pi(z+1/2)], \tag{28}$$

$$f_1(z)=\sum_{m=1}^M c_m\cos[(2m-1)\pi(z+1/2)]. \tag{29}$$

We have to truncate  $M$  in such a way that the solutions do not depend in any significant way on this parameter. Our criterion has been that the truncation value of  $M$  is sufficiently large such that  $\text{Nu}$  changes by less than 0.1% when  $M$  is replaced by  $M-5$ . The largest value for  $M$  used in the calculations was  $M=160$ . The relationships for  $w_1$  and  $\theta_1$  are symmetric with respect to  $z=0$  and the relationship for  $f_1$  is antisymmetric. The reason for this choice are the numerical investigations for the case of finite Prandtl number [21]. They show that with increasing Prandtl number, the fields  $w_1$  and  $\theta_1$  become symmetric with respect to  $z=0$  and the profile for  $f_1$  becomes antisymmetric.

As it can be seen from Eqs. (21)–(23), we restrict our investigation to the  $1-\alpha$  solution of the variational problem. In addition to the objective for testing the assumption of the analytical theory from [69] we have one more reason. As shown by Chan, Ref. [8], when  $\text{Ta}<O(R^{4/3})$ , the maximizing solution has finitely many modes. This is an important difference with respect to the case of a fluid of finite Prandtl number and without rotation for which the number of wave numbers of the maximizing solution can be infinite. Moreover, in the region of large  $R$  and  $\text{Ta}$  and when

$$R^{(4\cdot 2^k-3)/(3\cdot 2^k-2)}\leq\text{Ta}\leq R^{(8\cdot 2^k-3)/(6\cdot 2^k-2)}, \tag{30}$$

the maximizing solution has  $k+1$  modes. The region of validity of the single-wave-number solution from Ref. [69] is a subregion of the region (30) when  $k=0$ . Thus, according to Eq. (30), the  $1-\alpha$  solution has to be maximizing when  $\text{Ta}<O(R)^{5/4}$ , i.e., for almost the entire regions of large  $R$  and  $\text{Ta}$  investigated in this paper.

### III. BEHAVIOR OF THE OPTIMUM FIELDS

From the point of view of the analytical theory [69] if  $\text{Ta}\ll\alpha_1^4$ , we do not expect significant changes in the asymptotic behavior of the optimum fields in comparison to the case without rotation. After a transition region around  $\text{Ta}\propto\alpha_1^4$ , we can check the assumptions and results of the asymptotic theory for the case of intermediate rotation rates, i.e., for  $\alpha_1^4\ll\text{Ta}\ll\alpha_1^6$ . After a second transition region around  $\text{Ta}\propto\alpha_1^6$ , we can study the influence of strong rotation and check the analytical results when  $\text{Ta}$  is larger than  $\alpha_1^6$  or when  $\alpha_1\gg\text{Nu}$ . In order to compare the numerical investigations to the assumptions and results of the analytical asymptotic theory, we have to consider the investigated regions in the planes  $\text{Ta}-\alpha_1$  and  $\text{Ta}-R$ . These regions are shown in Fig. 1. The figure is obtained as follows. For panel (a), we fix the Taylor number and calculate the function  $\text{Nu}(\alpha_1)$  for several values of the Rayleigh number. We denote with filled circles the values of the wave number  $\alpha_1$  corresponding to the maximum of the Nusselt number for given values of  $R$  and  $\text{Ta}$ . As the Taylor number is fixed, we obtain straight lines of filled circles with increasing Rayleigh number. The optimum value of the wave number increases with increasing Rayleigh number and the last circle on the right-hand side of each straight line corresponds to the maximum value of Rayleigh number for, which we have been able to perform the calculation for the corresponding fixed value of the Taylor number. Panel (b) of Fig. 1 is produced in the same manner as panel (a) with the difference that we fix the Taylor number and plot with filled circles the Rayleigh numbers corresponding to optimum values of  $\alpha_1$  plotted in panel (a). Thus, for an example, the last circle of the bottom straight line in panel (a) corresponds to the last circle at the bottom straight line in panel (b).

Panel (a) of Fig. 1 shows that on the basis of the performed numerical calculations we can make conclusions about regions where  $\text{Ta}\ll\alpha_1^4$ ;  $\text{Ta}\propto\alpha_1^4$  and  $\alpha_1^4\ll\text{Ta}\ll\alpha_1^6$ , i.e., for the regions of weak rotation, first transition region, and the region of intermediate Taylor numbers. We see that in the

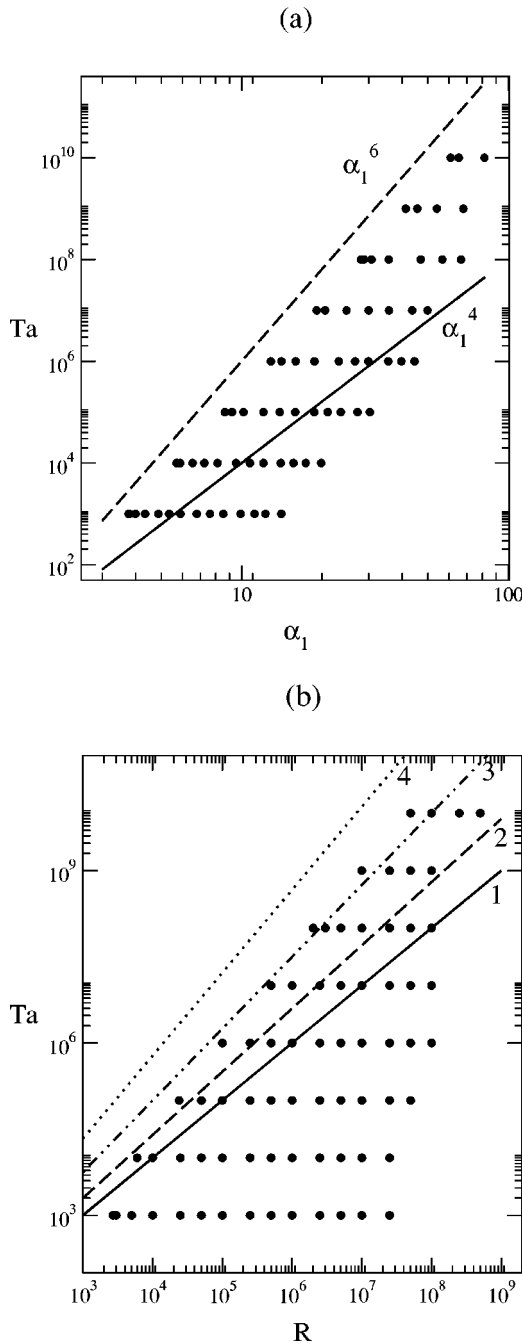


FIG. 1. Panel (a) investigated area for the optimum wave number. Solid line,  $Ta=\alpha_1^4$ ; dashed line,  $Ta=\alpha_1^6$ . Panel (b)  $R$ - $Ta$  diagram. Solid line denoted by 1,  $Ta=R$ ; dashed line denoted by 2,  $Ta=R^{11/10}$ ; dashed-double dotted line denoted by 3,  $Ta=R^{5/4}$ ; dotted line denoted by 4,  $Ta=R^{13/9}$ .

case of small Taylor numbers and increasing Rayleigh number, the wave number leaves the region of validity of the analytical asymptotic results and gets into the region of validity of the asymptotic results for the case without rotation. Only when the Taylor number becomes large enough, the numerical results can be compared to the analytical asymptotic results. In order to make statements about the analytical asymptotic relationships for the upper bound on the convective heat transport and optimal wave number we

have to take into account the region of validity of these bounds in the  $R$ - $Ta$  plane. It is presented in panel (b) of Fig. 1. For the case of three-layer optimum fields, the asymptotic bound for the case of intermediate Taylor numbers is valid for large enough values of the Rayleigh and Taylor numbers and when  $O(R)\ll Ta\ll O(R^{11/10})$ . As it can be seen from panel (b) of Fig. 1, the region of validity of asymptotic relationships is relatively small for the numerically reached values of  $R$  and  $Ta$ . Thus, we have to be careful in the statements about asymptotic relationships on the basis of the obtained numerical results. In the same panel, we present also the region  $R^{5/4}< Ta< R^{13/9}$ , where according to the theory of Chan, the two-wave-number solution has to be a maximizing one. We note that only few of our calculations are in this region of the  $R$ - $Ta$  plane. These calculations, however, are relatively close to the onset of convection and thus are quite far from the region where the asymptotic properties of this solution can be investigated. We estimate that in order to do this investigation, one has to perform numerical calculations for values of Rayleigh and Taylor numbers, at least  $10^{18}-10^{20}$ . This task requires much computing time even for the largest computers. Moreover, the results for the two-wave-number solution are not so important for the analytical multi-wave-number theory because all assumptions, made in order to construct such a theory, can be tested for much lower Rayleigh and Taylor numbers in the case of the single-wave-number theory.

One of the widely used assumptions of the asymptotic theory is that the ratio  $\Pi = w_1\theta_1/\langle w_1\theta_1 \rangle$  tends to 1 in the entire vertical region of the fluid layer except for the two boundary layers. Figure 2 shows the influence of Rayleigh and Taylor number on  $\Pi$ . In panel (a), the Taylor number has the fixed value  $Ta=10^3$  but the picture is characteristic also for the case of much larger Taylor numbers. We observe the formation of boundary layers and in large areas of the fluid layer  $\Pi\rightarrow 1$  as it is assumed in the analytical asymptotic theory. The effect of increasing rotation on  $\Pi$  can be seen in panel (b) of Fig. 2. Here the Rayleigh number is fixed. In the region of small Taylor numbers, we observe relatively slow deviation from a profile close to the asymptotic profile. This tendency becomes much visible when Taylor number becomes large enough and the profile becomes close to the profile around the onset of the convection. Thus, in order to have  $\Pi\rightarrow 1$  it is not sufficient that the values of Rayleigh and Taylor numbers are large enough. In addition, the Rayleigh number must be large enough for the given value of the Taylor number.

Let us fix the Taylor number and increase the Rayleigh number. This leads to formation of boundary layers of the optimum fields. Larger values of the Taylor number lead to more slow formation of boundary layers with increasing Rayleigh number. Figure 3 shows the formation of boundary layers for  $w_1(z)$  when  $Ta=10^6$ . We note that in the case of finite Prandtl numbers and without rotation, we observe a formation of a peak of the function dependent on  $w_1(z)$  and motion of this peak to the border of the fluid layer with increasing Rayleigh number [15]. Here the Prandtl number is infinite and there is no peak formation. Thus, the situation is analogous to the case without rotation [16] with one differ-

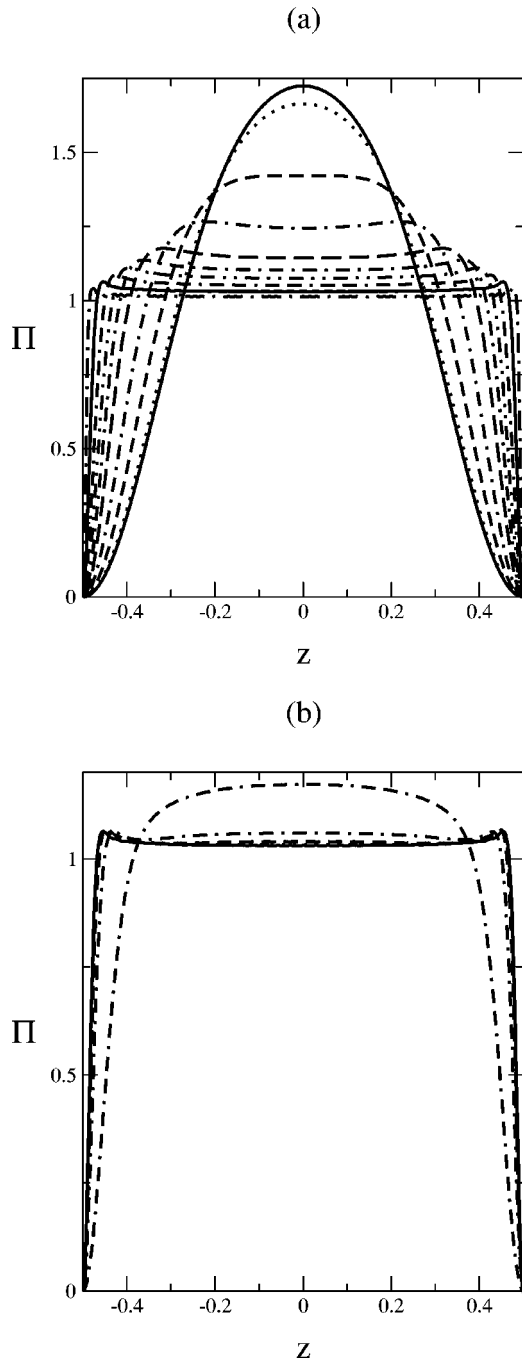


FIG. 2. Panel (a) influence of Rayleigh number on the ratio  $\Pi = \overline{w_1 \theta_1} / \langle w_1 \theta_1 \rangle$  when Taylor number is fixed,  $Ta = 10^3$ . From top to the bottom at  $z = 0$ :  $R = 2.7 \times 10^3, 3 \times 10^3, 5 \times 10^3, 10^4, 2.5 \times 10^4, 5 \times 10^4, 10^5, 2.5 \times 10^5, 10^6, 10^7$ . Panel (b) influence of Taylor number when Rayleigh number is fixed,  $R = 10^6$ . Solid line,  $Ta = 10^3$ ; dotted line,  $Ta = 10^4$ ; dashed line,  $Ta = 10^5$ ; dot-dashed line,  $Ta = 10^6$ ; dot-two dashes line,  $Ta = 10^7$ .

ence: because of the presence of rotation, the formation of boundary layers proceeds more slowly. Panel (b) of Fig. 3 shows that the increasing Taylor number when the Rayleigh number is fixed leads to vanishing of the boundary layers for  $w_1$  and to decreasing of the function  $w_1(z)$  in the entire vertical direction of the fluid layer.

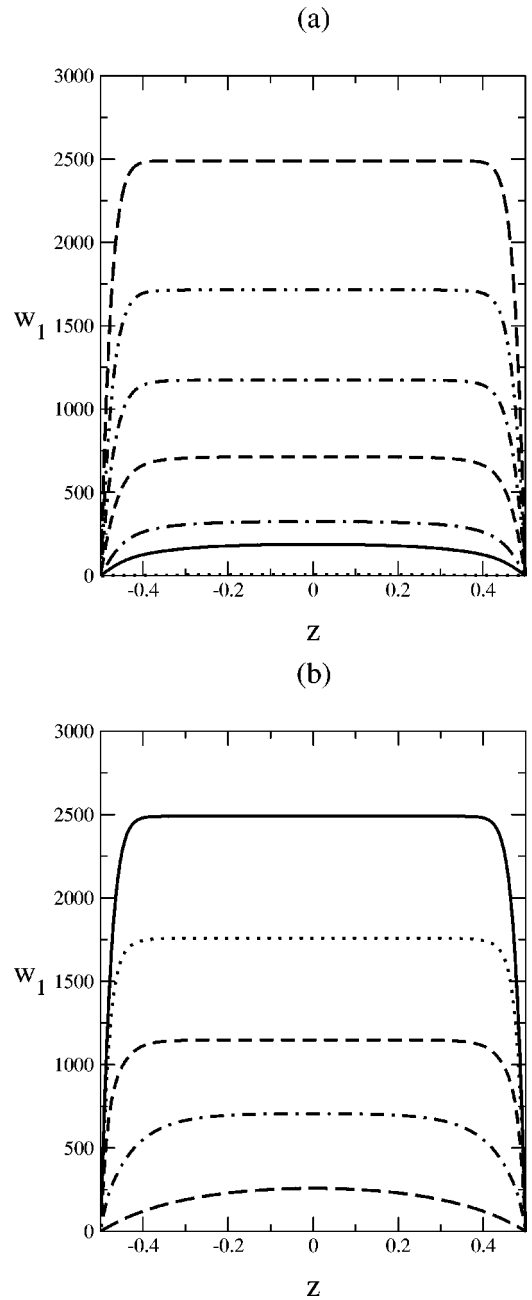


FIG. 3. Panel (a) influence of Rayleigh number on  $w_1$  when the Taylor number is fixed,  $Ta = 10^6$ . Solid line,  $R = 10^5$ ; dot-long dashed line,  $R = 10^6$ ; dashed line,  $R = 2.5 \times 10^6$ ; dot-short dashed line,  $R = 10^7$ ; two dots-dashed line,  $R = 2.5 \times 10^7$ ; long-dashed line,  $R = 10^8$ . Panel (b) influence of Taylor number on  $w_1(z)$  when Rayleigh number is fixed.  $R = 10^8$ . Solid line,  $Ta = 10^6$ ; dotted line,  $Ta = 10^7$ ; dashed line,  $Ta = 10^8$ ; dot-dashed line,  $Ta = 10^9$ ; long-dashed line,  $Ta = 10^{10}$ .

Characteristic feature of the field  $\theta_1$  is the fast formation of boundary layer with increasing Rayleigh number. The boundary layer is very thin and the corresponding peaks of the function  $\theta_1(z)$  are very sharp—see panel (a) of Fig. 4. We note that the boundary layer for  $\theta_1$  is thinner than the boundary layer for  $\Pi$ , which is thinner than the boundary layer for  $w_1$ . The presence of rotation leads to a

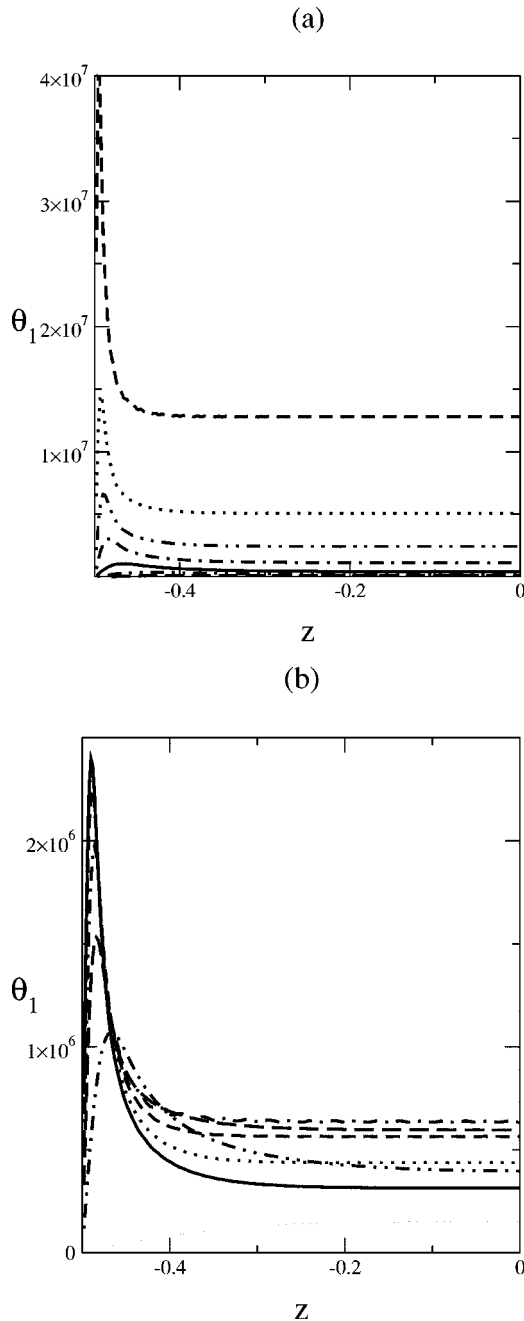


FIG. 4. Panel (a) influence of Rayleigh number on  $\theta_1$  when Taylor number is fixed.  $Ta = 10^8$ . From top to the bottom:  $R = 2.5 \times 10^8, 10^8, 5 \times 10^7, 2.5 \times 10^7, 10^7, 5 \times 10^6, 3 \times 10^6, 2 \times 10^6$ . Panel (b) influence of Taylor number on the optimum field  $\theta_1$ .  $R = 10^7$ . The values of the Taylor numbers are solid line,  $Ta = 10^3$ ; dotted line,  $Ta = 10^4$ ; dashed line,  $Ta = 10^5$ ; dot-dashed line,  $Ta = 10^6$ ; long dashed line,  $Ta = 10^7$ ; two dots-dashed line,  $Ta = 10^8$ .

delay of formation of the boundary layer. In large region of fluid layer, the deviations of  $\theta_1$  from its value at the interior of the layer are very small. The effect of vanishing of the boundary layer of  $\theta_1$  because of increasing rotation can be seen in panel (b) of Fig. 4. The peak in the boundary layer persists up to very large values of Taylor numbers. The decreasing value of  $\theta_1$  in the boundary layer is connected with increasing value of the optimum field in the interior of the

fluid layer. We note that the decrease in  $w_1$  and  $\theta_1$  when  $R$  is fixed and  $Ta$  increases leads to decrease in  $\langle w_1 \theta_1 \rangle$  and thus to decrease in the Nusselt number.

A new moment in comparison to the case without rotation is the presence and behavior of the field  $f_1(z)$ . Panel (a) of Fig. 5 shows the influence of increasing Rayleigh number on  $f_1$  when the Taylor number is fixed. We observe formation of a boundary layer and at the remaining part of the layer,  $f_1$  is very close to 0 as assumed by the analytical asymptotic theory. The Taylor number has quite an interesting influence on  $f_1(z)$ . This can be seen in panel (b) of Fig. 5. When the Taylor number is small in comparison to the Rayleigh number, the increase in rotation leads to formation of boundary layer and to enlarging the area in the interior of the fluid layer where  $f_1$  has a small value. However, further increasing in the Taylor number leads to the opposite process. The sharp boundary layer begins to smooth and the absolute value of  $f_1$  in the interior of the fluid layer increases.

Figure 6 presents the influence of the Taylor and Rayleigh numbers on the mean temperature profile as calculated by Eq. (9). The upper panel presents the case of fixed Rayleigh number. The profile of  $\bar{\Theta}$  has characteristic peaks that vanish when the Taylor number increases. The process of formation of such peaks can be seen when the Taylor number is fixed and Rayleigh number increases. The profiles shown in Fig. 6 could be used as hints for construction of background fields when applying the method of Doering and Constantin to the problems of rotating convection. These profiles show that the optimum background field could have complicated structure, consisting of curved lines.

#### IV. UPPER BOUNDS ON THE HEAT TRANSPORT AND BEHAVIOR OF THE OPTIMUM WAVE NUMBER

The influence of rotation on the optimum wave number is in agreement to the assumptions of the analytical asymptotic theory. Panel (a) of Fig. 7 shows that for fixed and small Taylor numbers,  $\alpha_1(R)$  follows the the power law for the case without rotation but the coefficient before the power is larger than 0.2. For example, when  $Ta = 10^3$ , the coefficient is close to 0.9. With increasing Taylor number,  $\alpha_1(R)$  is close to the asymptotic relationship  $\alpha_1 = (R/5)^{1/4}$  for the case with rotation but when the Rayleigh number becomes large enough after a transition region  $\alpha_1$  begins to follow the asymptotic relationship for the case without rotation [see, for example, the triangles marking the case  $Ta = 10^6$  in panel (a) of Fig. 7]. With increasing Taylor number the region, in which the asymptotic relationship for the case with rotation is followed becomes larger at the expense of the transition region and the region where  $\alpha_1$  is close to the asymptotic power law for the case without rotation. We note that this transition region is the transition region around  $Ta \propto \alpha_1^4$  predicted from the analytical theory.

Panel (b) of Fig. 7 presents the influence of Rayleigh and Taylor numbers on convective heat transport. We observe that increasing Taylor number leads to decreasing Nusselt number, i.e., to an inhibition of the heat transport. Thus, the optimum theory correctly reflects this property of the rota-

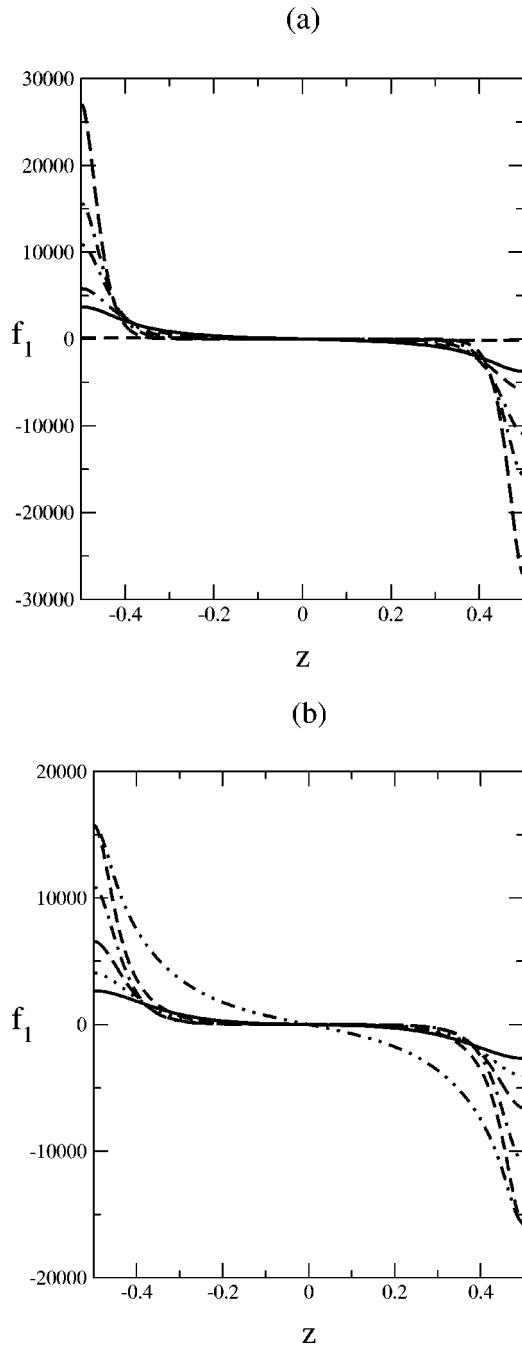


FIG. 5. Panel (a) influence of Rayleigh number on the field  $f_1(z)$  when Taylor number is fixed,  $Ta=10^6$ . From top to the bottom at  $z=-1/2$ :  $R=10^5, 10^6, 2.5 \times 10^6, 10^7, 2.5 \times 10^7, 10^8$ . Panel (b) influence of Taylor number on the optimum field  $f(z)$ .  $R=10^7$ . The values of the Taylor number are solid line,  $Ta=10^3$ ; dotted line,  $Ta=10^4$ ; long-dashed line,  $Ta=10^5$ ; dot-dashed line,  $Ta=10^6$ ; dashed line,  $Ta=10^7$ ; two dots-dashed line,  $Ta=10^8$ .

tion. For large Taylor numbers, the optimum fields converge very fast to the corresponding asymptotic profiles. This makes difficult their numerical investigation for large values of the  $R$  because of the very small sizes of the corresponding boundary layers. One of the assumptions of the analytical theory is that for small Taylor numbers, the upper bound on  $Nu$  should be close to the bound  $0.32R^{1/3}$  for the case with-

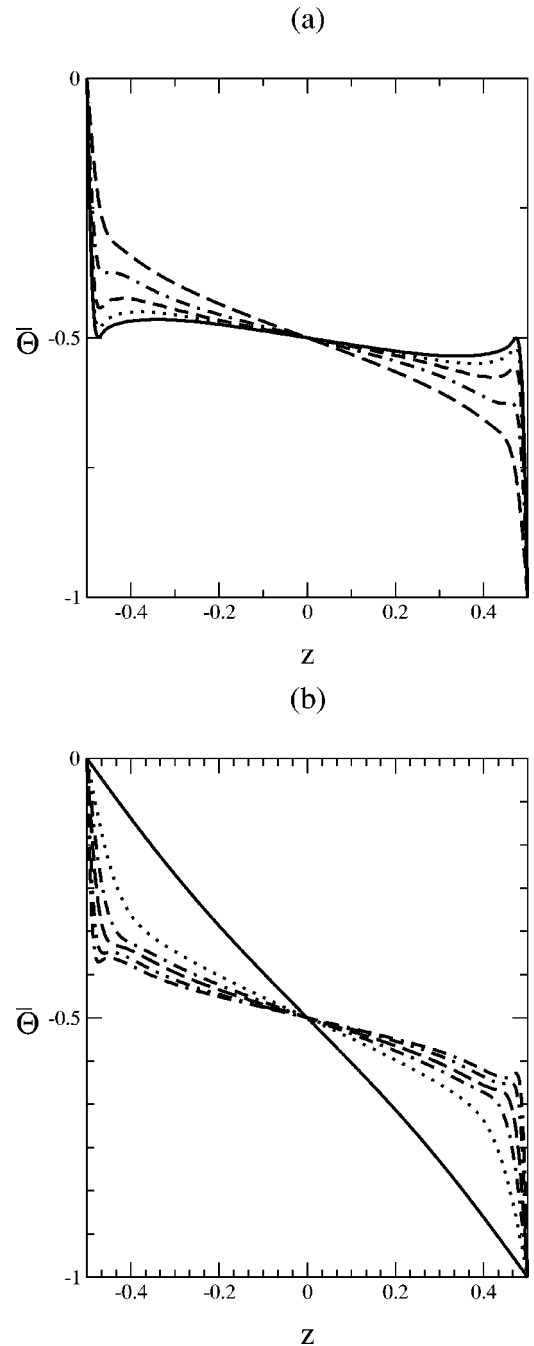


FIG. 6. Panel (a) influence of rotation on the mean temperature field,  $R=2.5 \times 10^6$ . Solid line,  $Ta=10^3$ ; dotted line,  $Ta=10^4$ ; dashed line,  $Ta=10^5$ ; dot-dashed line,  $Ta=10^6$ ; long-dashed line,  $Ta=10^7$ . Panel (b) influence of the Rayleigh number when Taylor number is fixed,  $Ta=10^6$ . Solid line,  $R=10^5$ ; dotted line,  $R=2.5 \times 10^5$ ; dot-dashed line,  $R=5 \times 10^5$ ; dashed line,  $R=10^6$ ; two dots-dashed line,  $R=2.5 \times 10^6$ ; dot-two dashes line,  $R=5 \times 10^6$ .

out rotation [16]. Indeed in panel (b) of Fig. 7, we see that with increasing Rayleigh number and fixed Taylor number, the upper bound on the convective heat transport approaches from below the above-mentioned bound.

We can compare the numerical bounds to the analytical bounds, obtained in Refs. [69,37,45]. A comparison between the analytical bounds from Refs. [69,37] has been made in

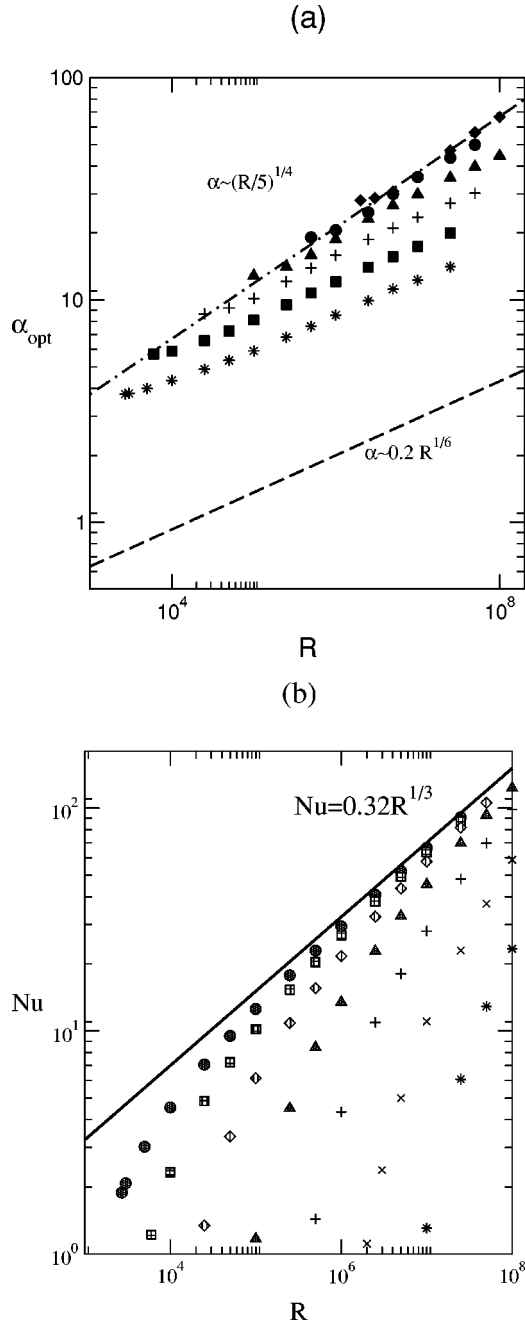


FIG. 7. Panel (a) influence of Taylor number on the optimum wave number. Dashed line: asymptotic optimum wave number for the case without rotation. Dot-dashed line: asymptotic optimum wave number for the case with rotation. Stars,  $Ta=10^3$ ; squares,  $Ta=10^4$ ; plusses,  $Ta=10^5$ ; triangles,  $Ta=10^6$ ; circles,  $Ta=10^7$ ; diamonds,  $Ta=10^8$ . Panel (b) Nusselt number as function of Rayleigh number for different Taylor numbers. Solid line: the asymptotic power law  $Nu=0.32R^{1/3}$  for the case without rotation. Circles,  $Ta=10^3$ ; squares,  $Ta=10^4$ ; diamonds,  $Ta=10^5$ ; triangles,  $Ta=10^6$ ; plusses,  $Ta=10^7$ ;  $\times$ ,  $Ta=10^8$ ; stars,  $Ta=10^9$ .

Ref. [69]. Due to this, we shall compare the bounds obtained above to the bounds from Refs. [69,45]. In Ref. [69], the bounds are as follows. For large values of  $R$  and  $Ta$  and when  $Ta \ll R$ , the situation is similar to the case without rotation and the upper bound is the same as in the nonrotational case:

$Nu=0.32R^{1/3}$  as obtained in Ref. [16]. After a transition region around  $Ta=R$  for the region  $O(R) \ll Ta \ll O(R^{11/10})$ , the bound is

$$Nu - 1 = \frac{2}{3^{1/3} 5^{5/3} D^{4/3}} \frac{R^{2/3}}{Ta^{1/5}} \left[ \left( \frac{5Ta^2}{R} \right) \right]^{1/3} L, \quad (31)$$

where  $D=1.06$  and  $L$  is

$$L = \left( 1 + \frac{\ln \left\{ \ln \left[ \left( \frac{5Ta^2}{R} \right)^{1/6} \right] \right\}}{3 \ln \left( \frac{5Ta^2}{R} \right)^{1/6}} \right)^{-1/3}. \quad (32)$$

There are three kinds of bounds in Ref. [45]. The bound without rotation

$$Nu < R^{1/3} (\ln R)^{2/3} \quad (33)$$

holds up to the  $Ta \leq 4R^{1/3} (\ln R)^{5/3}$ . The bound

$$Nu \leq \left( \frac{1}{2} \right)^{4/5} Ta^{2/5} R^{1/5} \quad (34)$$

has a region of validity  $4R^{1/3} (\ln R)^{5/3} \leq Ta \leq 4R^{1/2}$ , and finally the bound

$$Nu \leq R^{2/5} \quad (35)$$

is valid in the region  $4R^{1/2} \leq Ta \leq 4R^4$ .

Figure 8 shows a comparison among the numerical bounds and the above-mentioned analytical bounds. There are three groups of plots shown in this figure. The symbols (circles, squares, diamonds, triangles, and plusses) show the numerically obtained bounds. The dotted, dashed, and dot-dashed lines present the bound (35) for the same values of Rayleigh numbers, for which the numerical bounds are obtained. The solid line marked with  $B$  presents the bound (31) correspondent to the numerical bound, marked with plusses. The last numerical bound is about 70% lower than the bound (31). Figure 8 is a nice illustration of the fact that because of the large number of assumptions in the process of the analytical bounds in Ref. [69], their region of validity is much smaller in comparison to the region of validity of the numerical bounds. As in the all cases we investigated numerically up to now [16,20], the here obtained numerical bounds lie below the analytical asymptotic bounds.

The difference among the numerical bounds and the analytical bound (35) is larger than 70% but an useful feature of the bound (35) is that this bound has much larger region of validity than the bound (31). Thus it is the best analytical bound for the regions of  $R$  and  $Ta$  where the analytical bound (31) is not valid.

## V. CONCLUDING REMARKS

The processes in rotating convecting systems are governed by the interplay between heating and rotation, i.e., between the Rayleigh and Taylor numbers. One assumption of the asymptotic theory is that for very large values of the

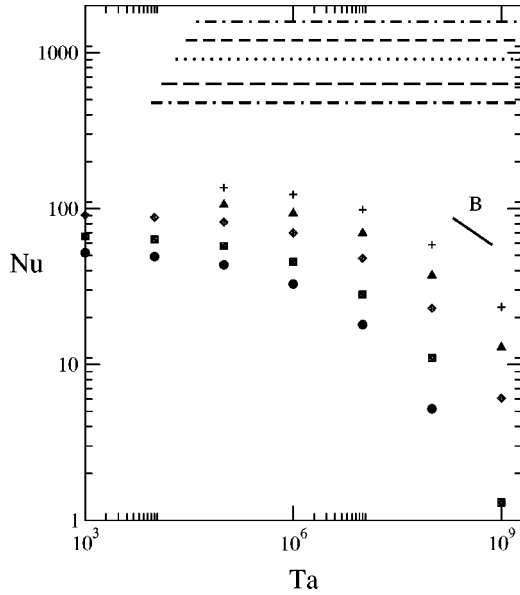


FIG. 8. Comparison of the numerically calculated relationship  $Nu(Ta)$  for fixed  $R$  and corresponding analytical asymptotic relationships from Refs. [45,69]. Nonmarked lines: analytical results from Ref. [45]. Double dash-dotted line,  $R = 5 \times 10^6$ ; long dashed line,  $R = 10^7$ ; dotted line,  $R = 2.5 \times 10^7$ ; dashed line,  $R = 5 \times 10^7$ ; dot-dashed line,  $R = 10^8$ . Solid line marked with  $B$ : analytical bound from Ref. [69] for  $R = 10^8$ . Symbols: numerical results obtained in this paper. Circles,  $R = 5 \times 10^6$ ; squares,  $R = 10^7$ ; diamonds,  $R = 2.5 \times 10^7$ ; triangles,  $R = 5 \times 10^7$ ; plusses,  $R = 10^8$ .

Rayleigh and Taylor numbers, some terms in the Euler-Lagrange equations are much smaller than the other terms. On the basis of this assumption, we neglect the influence of such terms and the equations are simplified. This allows one to obtain analytical asymptotic results for the upper bounds, wave numbers of the optimum fields, etc. For the case of nonasymptotic values of the Rayleigh and Taylor numbers, all terms in the Euler-Lagrange equations are significant, the equations become too complicated for an analytical treatment, and we have to solve them numerically. Because of the numerous assumptions for the behavior of the terms of the Euler-Lagrange equations of the variational problem, the region of applications of the analytical asymptotic results is confined in  $R$ - $Ta$  plane, and it is relatively small for intermediate values of Rayleigh and Taylor numbers accessible with computers. For an example, a more careful calculation of the coefficients in Eq. (30) leads to the following relationship for the validity of the single-wave-number solution for the case of large Rayleigh and Taylor numbers

$$\frac{2^{10}}{\pi^4} R \leq Ta \leq \frac{1}{5} R^{5/4}, \quad (36)$$

i.e., its region of validity starts when  $R$  becomes larger than 763 300. In the same way, the region of validity of the bound (34) begins when  $R^{1/6} \geq (\ln R)^{5/3}$ . In the case of numerical investigation, we do not make any assumptions about the Euler-Lagrange equations. This allows us to investigate up-

per bounds on the convective heat transport also in regions of Rayleigh and Taylor numbers where the assumptions of the asymptotic theory are not valid.

With respect to the assumptions of the analytical theory, we can make the following conclusions.

(i) The numerical investigations confirm the assumption that in the case of small Taylor numbers, i.e., when  $Ta \ll \alpha_1^4$ , the behavior of the optimum fields and the behavior of the upper bounds is similar to the behavior in the case without rotation. In particular, the power law for  $\alpha_1$  is the same as in the case without rotation with the difference that the coefficient before the power is larger. For fixed values of Taylor number, and with increasing Rayleigh number the upper bound on  $Nu$  is close to the corresponding bound for the case without rotation.

(2) We detected the predicted transition region  $Ta \propto \alpha_1^4$  in the function  $\alpha(R, Ta)$ .

(3) When  $R$  and  $Ta$  are large enough then  $\Pi \rightarrow 1$  in the entire fluid layer except for the two boundary layers.

(4)  $w_1$  and  $\theta_1$  tend to be constants in the interior of the fluid layer and  $f_1 \rightarrow 0$  in the interior for large  $R$  and  $Ta$ .

(5) We observe different speeds of approaching of asymptotic relationships. There exist fast approaching of the asymptotic law for  $\alpha_1(R)$ . Much slower is the approaching the asymptotic relationship for the Nusselt number for the case of large Taylor number.

(6) The obtained numerical bounds are always lower than the analytical bounds, projected back to the intermediate values of  $R$  and  $Ta$ .

In addition, we observed interesting behavior of the vertical component of the vorticity where rotation can lead to formation of boundary layers. The optimum profiles for  $\bar{\Theta}$  are quite complicated. We note that these optimum profiles are obtained automatically on the basis of the calculated optimum fields and carry much interest for theoreticians and experimentalists information about the temperature distribution.

Finally, we note that our investigation was based on three-layer optimum fields, i.e., the optimum fields have the same structure as in the case without rotation. The numerical investigation in this paper confirms all assumptions of the corresponding analytical asymptotic theory. Thus, the way for amending the multi-wave-number theory of the upper bounds for the rotating convection is paved. In addition to this problem, the optimum theory of turbulence of rotating convection leads to many other interesting problems. For an example, in the case of infinite Prandtl numbers and rigid boundaries, the optimum fields have to be a four-layer one. Four-layers optimum fields could exist also for the case of stress-free boundaries. The investigations of these cases will be subject of future research.

#### ACKNOWLEDGMENTS

The author is grateful to Professor F. H. Busse for the stimulating discussions and to NATO for the support from its Cooperative Science and Technology Sub-Program through Grant No. PST.CLG.979126.

- [1] W.V.R. Malkus, Proc. R. Soc. London, Ser. A **225**, 185 (1954).  
 [2] W.V.R. Malkus, Proc. R. Soc. London, Ser. A **225**, 196 (1954).  
 [3] L.N. Howard, J. Fluid Mech. **17**, 405 (1963).  
 [4] F.H. Busse, J. Fluid Mech. **37**, 457 (1969).  
 [5] S.K. Chan, Stud. Appl. Math. **50**, 13 (1971).  
 [6] L.N. Howard, Annu. Rev. Fluid Mech. **4**, 473 (1972).  
 [7] V.P. Gupta and D.D. Joseph, J. Fluid Mech. **57**, 491 (1973).  
 [8] S.-K. Chan, J. Fluid Mech. **64**, 477 (1974).  
 [9] C. Hunter and N. Riahi J. Fluid Mech. **72**, 433 (1975).  
 [10] F.H. Busse, Adv. Appl. Mech. **18**, 77 (1978).  
 [11] F. H. Busse, in *Energy Stability and Convection*, edited by G. P. Galdi and B. Straughan (Pitman, Boston, 1988).  
 [12] F. H. Busse, in *Nonlinear Physics of Complex Systems*, edited by J. Parisi, S. C. Müller, and W. Zimmermann (Springer, Berlin, 1996).  
 [13] R.R. Kerswell and A.M. Soward, J. Fluid Mech. **328**, 161 (1996).  
 [14] R.R. Kerswell, J. Fluid Mech. **321**, 335 (1996).  
 [15] N.K. Vitanov and F.H. Busse, ZAMP **48**, 310 (1997).  
 [16] N.K. Vitanov, Phys. Lett. A **248**, 338 (1998).  
 [17] N.K. Vitanov and F.H. Busse, ZAMM **78**, S788 (1998).  
 [18] N.K. Vitanov, Phys. Rev. E **61**, 956 (2000).  
 [19] N.K. Vitanov, Eur. Phys. J. B **15**, 349 (2000).  
 [20] N.K. Vitanov, Physica D **136**, 322 (2000).  
 [21] N.K. Vitanov and F.H. Busse, Phys. Rev. E **63**, 016303 (2001).  
 [22] N.K. Vitanov, Eur. Phys. J. B **23**, 249 (2001).  
 [23] C.R. Doering and P. Constantin, Phys. Rev. Lett. **69**, 1648 (1992).  
 [24] R. Nicodemus, S. Grossmann, and M. Holthaus, Physica D **101**, 178 (1997).  
 [25] C.R. Doering and P. Constantin, Phys. Rev. E **49**, 4087 (1994).  
 [26] P. Constantin and C.R. Doering, Phys. Rev. E **51**, 3192 (1995).  
 [27] C.R. Doering and P. Constantin, Phys. Rev. E **53**, 5957 (1996).  
 [28] C.R. Doering and J.M. Hyman, Phys. Rev. E **55**, 7775 (1997).  
 [29] C.R. Doering and P. Constantin, J. Fluid Mech. **376**, 263 (1998).  
 [30] R. Nicodemus, S. Grossmann, and M. Holthaus, Phys. Rev. Lett. **79**, 4170 (1997).  
 [31] R. Nicodemus, S. Grossmann, and M. Holthaus J. Fluid Mech. **363**, 281 (1998).  
 [32] R. Nicodemus, S. Grossmann, and M. Holthaus, Eur. Phys. J. B **10**, 385 (1999).  
 [33] R. Nicodemus, S. Grossmann, and M. Holthaus, J. Fluid Mech. **363**, 301 (1998).  
 [34] N. Hoffmann and N.K. Vitanov, Phys. Lett. A **255**, 277 (1999).  
 [35] R.R. Kerswell, Physica D **100**, 355 (1997).  
 [36] R.R. Kerswell, Physica D **121**, 175 (1998).  
 [37] P. Constantin, C. Hallstrom, and V. Putkaradze, Physica D **125**, 275 (1999).  
 [38] R.R. Kerswell, Phys. Rev. E **59**, 5482 (1999).  
 [39] R.R. Kerswell, Phys. Lett. A **272**, 230 (2000).  
 [40] R.R. Kerswell, Phys. Fluids **13**, 192 (2001).  
 [41] C.R. Doering, E.A. Spiegel, and R.A. Worthing, Phys. Fluids **13**, 192 (2001).  
 [42] C.P. Caulfield and R.R. Kerswell, Phys. Fluids **13**, 894 (2001).  
 [43] R.A. Worthing, J. Fluid Mech. **431**, 427 (2001).  
 [44] C.R. Doering and P. Constantin, J. Math. Phys. **42**, 784 (2001).  
 [45] P. Constantin, C. Hallstrom, and V. Poutkaradze, J. Math. Phys. **42**, 773 (2001).  
 [46] P. Constantin and C.R. Doering, J. Stat. Phys. **94**, 159 (1999).  
 [47] J.A. Krommes and R.A. Smith, Ann. Phys. (N.Y.) **177**, 246 (1987).  
 [48] C.B. Kim and J.A. Krommes, J. Stat. Phys. **53**, 1103 (1988).  
 [49] C.B. Kim and J.A. Krommes, Phys. Rev. A **42**, 7487 (1990).  
 [50] C.Y. Wang, A. Bhattacharjee, and E. Hameiri, Phys. Fluids B **3**, 715 (1991).  
 [51] C.Y. Wang and A. Bhattacharjee, Phys. Fluids B **3**, 3462 (1991).  
 [52] C.B. Kim, Phys. Rev. E **55**, 2048 (1997).  
 [53] J.A. Krommes, Phys. Rep. **283**, 5 (1997).  
 [54] Y. Nakagava and P. Frenzen, Tellus **7**, 1 (1955).  
 [55] G. Veronis, J. Fluid Mech. **31**, 113 (1968).  
 [56] G. Küppers and D. Lortz, J. Fluid Mech. **35**, 609 (1969).  
 [57] H.T. Rossby, J. Fluid Mech. **36**, 309 (1969).  
 [58] R.C.F. Somerville and F.B. Lipps, J. Atmos. Sci. **30**, 590 (1973).  
 [59] F.H. Busse, Rep. Prog. Phys. **41**, 1929 (1978).  
 [60] R.M. Clever and F.H. Busse, J. Fluid Mech. **94**, 609 (1979).  
 [61] B. M. Boubnov and G.S. Golitsyn, J. Fluid Mech. **219**, 215 (1990).  
 [62] H.J.S. Fernando, R. Chen, and D.L. Boyer, J. Fluid Mech. **228**, 513 (1991).  
 [63] R.E. Ecke, F. Zhong, and V. Steinberg, Phys. Rev. Lett. **67**, 2473 (1991).  
 [64] F. Zhong, R.E. Ecke, and V.E. Steinberg, J. Fluid Mech. **249**, 135 (1993).  
 [65] K. Julien, S. Legg, J. McWilliams, and J. Werne, J. Fluid Mech. **322**, 243 (1996).  
 [66] Y. Liu and R.E. Ecke, Phys. Rev. Lett. **79**, 2257 (1997).  
 [67] Y.T. Ker, Y.H. Li, and T.F. Lin, Int. J. Heat Mass Transf. **41**, 1445 (1998).  
 [68] P. Vorobieff and R.E. Ecke, Physica D **123**, 153 (1998).  
 [69] N.K. Vitanov, Phys. Rev. E **62**, 3581 (2000).  
 [70] S. Chandrasekhar, *Hydrodynamic and Hydromagnetic Stability* (Dover, New York, 1981).